Pergamon

Acta mater. 48 (2000) 4635–4640

Acta MATERIALIA

www.elsevier.com/locate/actamat

MODELING AND SIMULATION OF GRAIN GROWTH IN Si_3N_4. III. TIP SHAPE EVOLUTION

M. KITAYAMA[1]*, K. HIRAO[2], M. TORIYAMA[2] and S. KANZAKI[2]

[1]Synergy Ceramics Laboratory, Fine Ceramics Research Association, 2268-1 Shimo-Shidami, Moriyama-ku, Nagoya, AICHI 463-8687, Japan and [2]National Industrial Research Institute of Nagoya, 2268-1 Shimo-Shidami, Moriyama-ku, Nagoya, AICHI 463-8687, Japan

Abstract—Simulations based on the anisotropic Ostwald ripening model have been performed for the tip shape evolution of the β-Si_3N_4 crystal in the liquid phase. It was found that tip shape is a function of the liquid concentration and the relationship between the interfacial reaction and diffusion constants. Depending on the concentration of the liquid phase, a convex, almost flat, or concave surface appeared at the tip surface. The following two factors are crucial for understanding the development of concavity at the tip surface of the β-Si_3N_4 crystal: (1) strong growth anisotropy of the β-Si_3N_4 crystal that is the interfacial reaction and diffusion controlled kinetics of the (100) and (001) surfaces, respectively, and (2) supersaturation of the liquid phase.

Keywords: Grain growth; Kinetics; Tip shape evolution

1. INTRODUCTION

Anisotropic grain growth is the factor that makes silicon nitride (Si_3N_4) a unique and tough ceramic. Controlling its microstructure is crucial for improving its mechanical properties [1, 2] and is the reason why so many researchers have focused on understanding the mechanism of anisotropic grain growth in this material [3–16]. Recently, we proposed a thermodynamic model for anisotropic Ostwald ripening [17], and extended it to the α–β transformation [18]. Grain growth simulations based on this model were performed to analyze the effects of various kinetic parameters on grain growth of β-Si_3N_4. These works provided explanations for the puzzling experimental results obtained in previous works, such as the reduction of aspect ratio during Ostwald ripening [12–14, 19–21], and growth exponents higher than 3 [8, 22]. Although in this study the macroscopic morphology evolution, i.e. the evolution of aspect ratio (length/width) and its distribution, was considered, the microscopic morphology, i.e. the real crystal shape, was not examined.

The β-Si_3N_4 crystal grown in the liquid phase is known to have a strong tendency to show an atomically flat interface, namely a facet, along the (100) prismatic plane. Periodic bond chain (PBC) analysis predicted the growth morphology of the β-Si_3N_4 crystal which consisted of the {100} prism and {101} pyramid habit planes, and demonstrated that the elongated hexagonal rod shape is the intrinsic morphology of the β-Si_3N_4 crystal [23]. The fact that the {100} plane has by far the lowest attachment energy means that nucleation on this plane has a high activation energy. As a result, an atomically flat interface would appear along this plane, and interfacial reaction controlled growth in the [210] direction is expected. However, the attachment energy of the {101} plane is not as low as that of the {100} plane, and the activation energy for nucleation on this plane is expected to be lower than that of the {100} plane. Thus, it would be difficult to predict whether the growth kinetics in the [001] direction are diffusion controlled or interfacial reaction controlled. According to their analysis, if the growth unit has PBC vectors [010] and [001], an atomically rough interface would appear at the tip of the β-Si_3N_4 crystal, and thus diffusion controlled grain growth would be predicted in this direction. The {101} and/or {001} interface, a slightly curved interface close to the {001} plane [23], and a round, atomically rough interface [3] were all observed at the tip of the β-Si_3N_4 crystal under different experimental conditions.

It is generally accepted that a convex and round (spherical) shape appears when growth kinetics is controlled by diffusion. This is believed to be so even

* To whom all correspondence should be addressed. Tel.: +81-92-606-3131 2455; fax: +81-92-606-0728.
E-mail address: kitayama@fit.ac.jp (M. Kitayama)

1359-6454/00/$20.00
PII: S1359-6454(00)00250-0

in the anisotropic case, in which growth in a certain direction is controlled by interfacial reaction [24]. However, a recent experimental result demonstrated a very different picture [25]. It was found that the tip shape of the hexagonal β-Si_3N_4 crystal grown in the liquid phase was concave, and that its curvature related to the width of the crystal. The fact that such a highly non-equilibrium shape does exist is indicative of a driving force for mass transport other than curvature, and could be due to kinetics. Combining this and the previous results, it is expected that the kinetic parameters could significantly affect the tip shape of the β-Si_3N_4 crystal.

The aim of this work is to perform microscopic simulations for the morphology evolution of the β-Si_3N_4 crystal in the liquid phase based on the anisotropic Ostwald ripening model [17], to analyze the effect of various kinetic parameters on the tip shape evolution, and to provide a plausible reason for the development of concavity at the tip surface of the β-Si_3N_4 crystal.

2. SIMULATION PROCEDURE

The simulation is based on a two-dimensional, rectangular vessel filled with the liquid phase and containing a two-dimensional, rectangular crystal with (100) side and (001) end surfaces. The width and length of the crystal are a and c, respectively. The size of the vessel is $c\times 2c$, and the crystal is located in the center of the vessel. Only half of this system is considered, so the size of the vessel for the purpose of the simulations is a square $c\times c$. Figure 1 shows the initial configuration for performing simulations. The simulation area is divided into a square lattice with a lattice parameter δ. Mass in the liquid phase can transfer by diffusion between two lattice points only in the x and y directions as shown in Fig. 1. Mass transfer is not allowed in the bulk and at the surface of the crystal (no volume or surface diffusion). Mass transfer at the solid–liquid interface is driven by the chemical potential difference between them. The chemical potential of the crystal surface μ_c is given by

$$\mu_c = \mu_0 + \kappa_c^{\gamma} \boldsymbol{V} \tag{1}$$

where μ_0, κ_c^{γ} and $\boldsymbol{V}$ are the standard chemical potential, weighted mean curvature (wmc) of the crystal surface [26], and molar volume of the crystal, respectively. In this work, the interfacial energy γ is assumed to be equal for all crystal surfaces. Figure 2 illustrates some examples of wmc for various crystal surfaces. Following the formulations used in the previous work [18], a diffusion controlled growth equation for one lattice point at the crystal surface can be expressed as follows

$$v = \frac{D_l}{\Delta x}\left\{\left(\frac{S_l}{S_\infty}-1\right)-\frac{\boldsymbol{V}}{RT}\kappa_c^{\gamma}\right\} \tag{2}$$

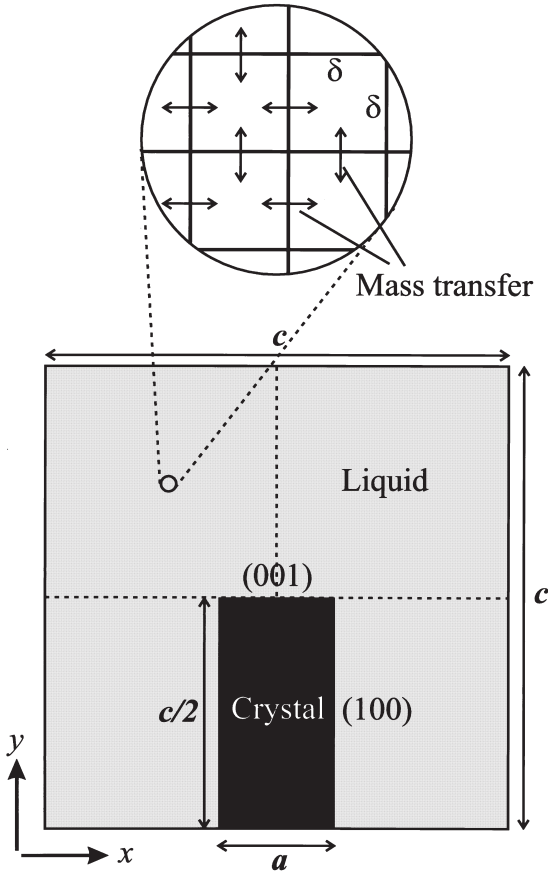

Fig. 1. Initial configuration for performing simulations. The width and length of the crystal are a and c, respectively. The simulation area, a square $c\times c$, is divided into a square lattice with a lattice parameter δ. Mass in the liquid phase can transfer by diffusion between two lattice points only in the x and y directions.

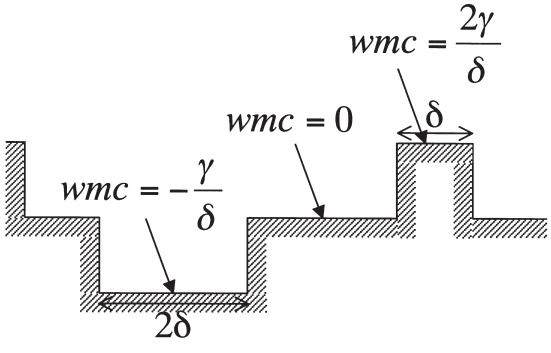

Fig. 2. Examples of wmc for various crystal surfaces.

where v, D_l, Δx, S_l and S_∞ are the normal velocity of the interface motion, diffusion constant in the liquid phase, diffusion distance, concentration in the liquid phase, and the solubility of the crystal with an infinite size, respectively, and R and T have the usual meanings. Likewise, an interfacial reaction controlled growth equation can be expressed as follows

$$v = K\left\{\left(\frac{S_l}{S_\infty}-1\right)-\frac{V}{RT}\kappa_c^\gamma\right\} \tag{3}$$

where K is the interfacial reaction constant, and it must be $D/\Delta x \gg K$ to be interfacial reaction controlled kinetics. The basic assumption in this work is that growth is controlled by diffusion and interfacial reaction in the [001] and [100] directions, respectively.

3. RESULTS AND DISCUSSION

3.1. Parameters

The activation energy E_d of diffusion for the Si_3N_4–SiO_2–Y_2O_3 system was determined by Babini et al. [27] to be 545 kJ/mol. The pre-exponent constant for diffusion D_0, taken from the one that showed good agreement with the known grain growth data obtained for β-Si_3N_4 in a previous work [17], has the value 1 m^2/s. The diffusion distance is equal to the lattice constant δ for simulation, and is 0.02 μm. Annealing temperature is 1600°C. Thus, in this work the diffusion constant has a value of about 6.21×10^{-16} m^2/s. The interfacial energy γ between the β-Si_3N_4 crystal and the liquid phase is 0.3 J/m^2 unless otherwise mentioned. The concentration of the β-Si_3N_4 crystal in the liquid phase C_β was set to 0.2, and is a good approximation according to the phase diagram of the Si_3N_4–SiO_2–Y_2O_3 system [28]. The width a and length c of the β-Si_3N_4 crystal were set to 1 μm and 4 μm, respectively, unless otherwise mentioned. In most cases, the interfacial reaction constant K was set to zero, which means no growth in the [100] direction, except when the ratio R of the interfacial reaction constant K and diffusion constant/diffusion distance $D/\Delta x$ is changed.

3.2. Effect of the liquid concentration

For the first simulation the liquid concentration C was set to 0.21, which means that the liquid phase was supersaturated. Figure 3 shows the time evolution of the tip shape of the β-Si_3N_4 crystal in the liquid phase. Starting from the initial configuration shown in Fig. 1, crystal shapes at the annealing times of 10 000, 20 000 and 40 000 s are shown in this figure. The black shape located at $x = 0$ is the β-Si_3N_4 crystal that is surrounded by the liquid phase. The concentration of the liquid phase is expressed by shading: the lighter the shading, the lower the concentration. Initially a flat surface of the (001) plane of the β-Si_3N_4 crystal develops concavity with time. In fact, the center of the tip is concave, while the edge of the tip is convex. This variation in curvature is consistent with experimental observations [25]. It creates mass flow from the edge to the center along the tip surface. This further suggests that mass constantly flows from the side (100) surface to the tip (001) surface. Since the wmc of the (100) and (001) surfaces, κ^γ_{100} and κ^γ_{001}, are $2\gamma/c$ and $2\gamma/a$, respectively, it becomes $\kappa^\gamma_{100}<\kappa^\gamma_{001}$ when $c>a$ as usually is the case for the elongated β-Si_3N_4

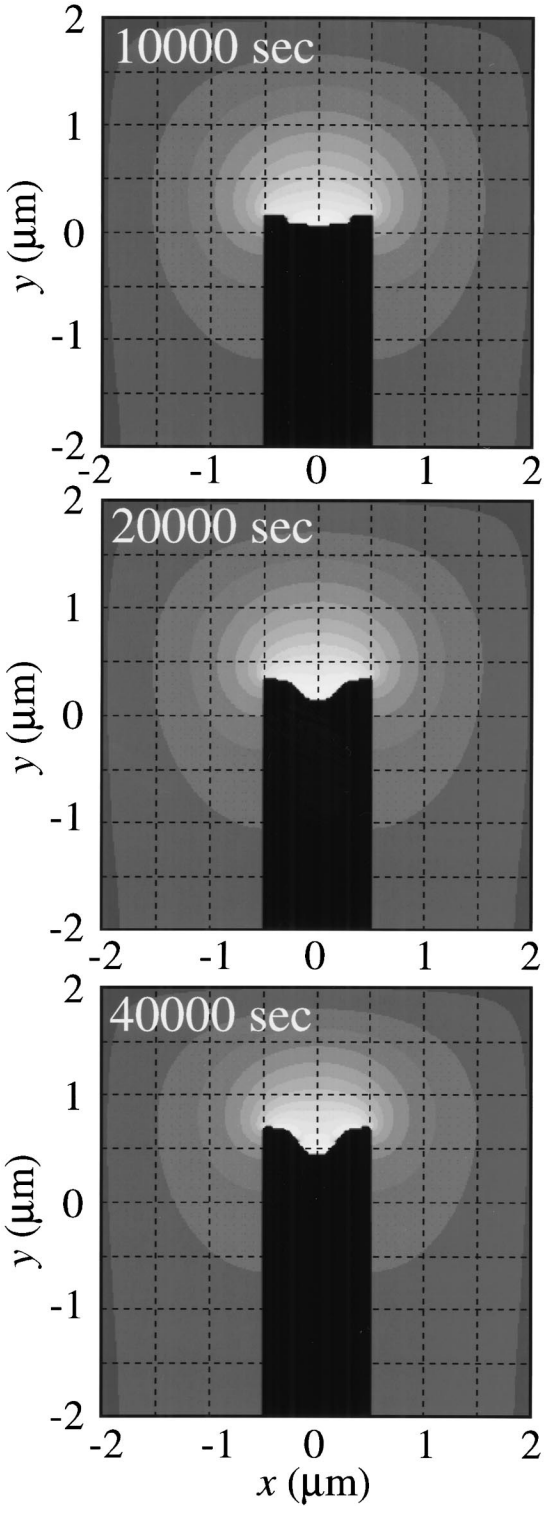

Fig. 3. Time evolution of the tip shape of the β-Si_3N_4 crystal in the liquid phase. Crystal shapes after 10 000 s (top), 20 000 s (middle), and 40 000 s (bottom) are shown.

crystal. From equation (1), the chemical potential of the (100) surface is lower than that of the (001) surface, and it drives mass transport from the (001) surface to the (100) surface. This does not agree with the opposite mass flow expected from the concavity at the tip, and suggests that mass flow must be driven by a force other than the surface tension. We can expect that this force would be derived from the supersaturation in the liquid phase. In this simulation, the liquid phase is slightly supersaturated. Since growth in the [001] direction is controlled by diffusion, a concentration gradient with an almost spherical shape is observed around the tip. This results in the lowest concentration point (the lightest shade in the figure) at the center of the tip ($x = 0$). In contrast, there is almost no concentration gradient in the direction normal to the (100) surface due to the interfacial reaction controlled kinetics (no growth in this case), especially at the center of the (100) surface ($y = -2$), which means that the concentration at this point is as high as that at the point far from the crystal ($x = \pm 0.5$, $y = -2$). As a result, a concentration gradient develops along the (100) surface from the center ($y = -2$) to the tip ($y = 0$), which drives mass flow from the side surface to the tip surface. Because the concentration at the edge of the tip ($x = \pm 0.5$) is higher than at the center ($x = 0$), the growth rate at the edge is also higher than at the center. This is the reason for the development of concavity at the tip. However, as the edge grows in the [001] direction, the chemical potential around the edge point of the tip surface increases, and finally reaches a steady-state. This determines the shape of the tip in a steady-state. Because the change of tip shape occurs mainly during the initial 20 000 s, and those after 20 000 and 40 000 s are nearly identical, we could say that the tip shape after 40 000 s is close to the one in a steady-state.

Figure 4 demonstrates the effect of liquid concentration on tip shape. The concentration of the liquid phase C varied from 0.19 (non-saturated) to 0.20 (saturated) to 0.21 (supersaturated). All results are obtained after 40000 s. As expected, convex, almost flat, and concave surfaces are developed at the tip in the cases of $C = 0.19$, 0.20 and 0.21, respectively. Consequently, we conclude that the concavity at the tip is attributed to supersaturation of the liquid phase. This variation in curvature due to the liquid concentration could explain the variety of the tip shapes observed experimentally: a round (convex) shape [3], a slightly curved surface close to the [001] plane [16], and a concave shape [25].

3.3. Effect of crystal width

It was discovered that concavity at the tip depended on crystal width: the larger the width of the crystal, the more concavity it developed [25]. To investigate the effect of crystal width on tip shape, simulations were performed in which crystal width, a, was changed from 0.5 to 1.0–1.5 μm. Other parameters remained the same as in the previous simulations.

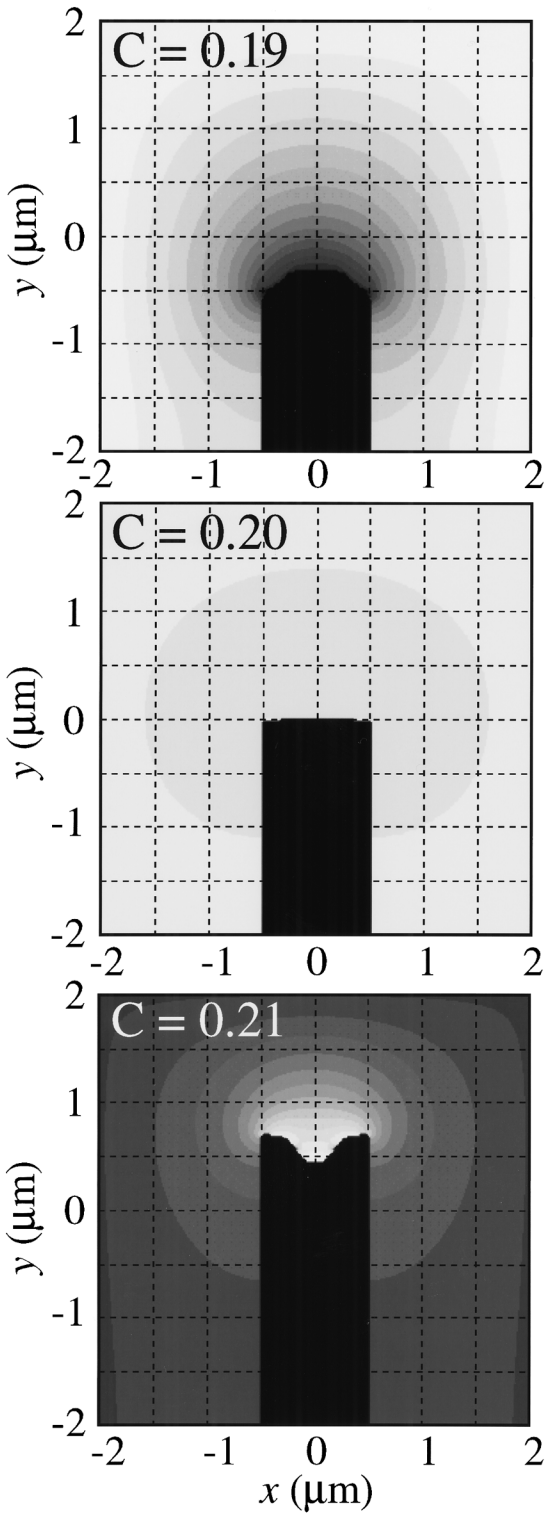

Fig. 4. Effect of liquid concentration on tip shape. The concentration of the liquid phase C varied from 0.19 (non-saturated, top) to 0.20 (saturated, middle) to 0.21 (supersaturated, bottom). All results are obtained after 40 000 s.

Figure 5 shows the shapes of the crystal after 40 000 s. The trend mentioned above can be clearly observed in these figures and is a result of different distances from the edge to the center at the tip surface. Since mass arrives from the edge to a large extent, it is gradually consumed during motion to the center along the tip surface due to diffusion-controlled growth in the [001] direction. When this distance is short, the concentration difference between the edge and the center is small and less concavity develops, as observed in the case of $a = 0.5$ (μm) and vice versa in the case of $a = 1.5$ (μm).

3.4. Effect of the kinetic parameter

Simulations have been performed so far setting the interfacial reaction constant at the (100) surface $K = 0$ to make them simple. We have understood in the above discussions that it is strong growth anisotropy and supersaturation in the liquid phase that make the tip shape concave. Thus, it is of great interest to see the effect of the relationship between the interfacial reaction constant K and the diffusion constant D_l. To directly compare them, the diffusion constant must be divided by the average diffusion distance Δx. Here, Δx is assumed to be equal to half the crystal width, $a/2$ [29]. Simulations are performed changing the ratio $R = K/(D_l/\Delta x)$ from 0.01 to 0.05 to 0.25. Other parameters are the same as in the previous simulations. Figure 6 shows the tip shapes in these cases after 40 000 s. It is clearly seen that the concentration gradient (corresponding to the number of shades), and hence growth rate, increase in the [100] direction as R increases. Almost no width growth is observed when $R = 0.01$, while a significant growth is recognized when $R = 0.25$. The most prominent difference among these cases is the concavity at the tip. The greater the R value becomes (the more the growth in the [100] direction becomes diffusion-controlled), the less concavity develops at the tip. In the previous section, we observed that concavity at the tip became greater with the increases of width. Figure 6 demonstrates that the effect of kinetic parameters overcomes the effect of width. Thus, we have confirmed that strong growth anisotropy is the key to understanding the development of concavity at the tip surface of the β-Si_3N_4 crystal.

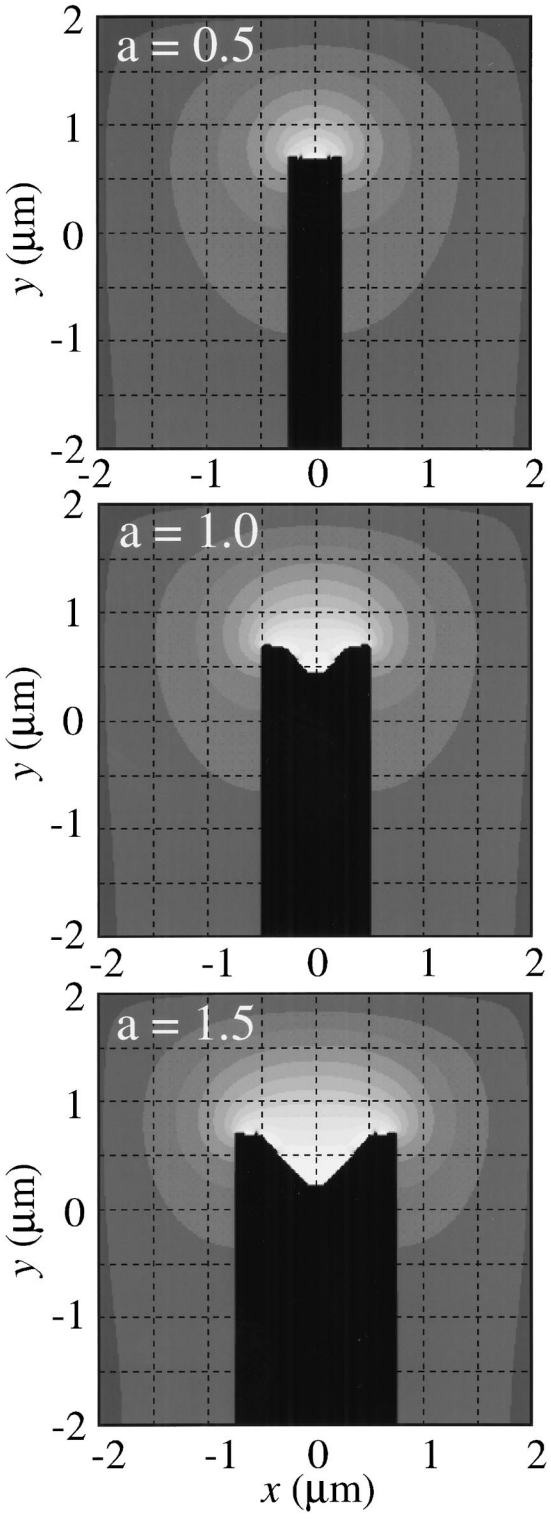

Fig. 5. Effect of crystal width on tip shape. Simulations are performed changing the crystal width a from 0.5 μm (top) to 1.0 μm (middle) to 1.5 μm (bottom). All results are obtained after 40 000 s.

4. CONCLUSION

Simulations based on the anisotropic Ostwald ripening model have been performed for the tip shape evolution of the β-Si_3N_4 crystal in the liquid phase. It has been found that tip shape is a function of liquid concentration and the relationship between the interfacial reaction and diffusion constants. The following conclusions can be drawn based on this work.

1. The variety of tip shapes observed experimentally, a round (convex) shape, a slightly curved surface close to the [001] plane, and a concave shape, are

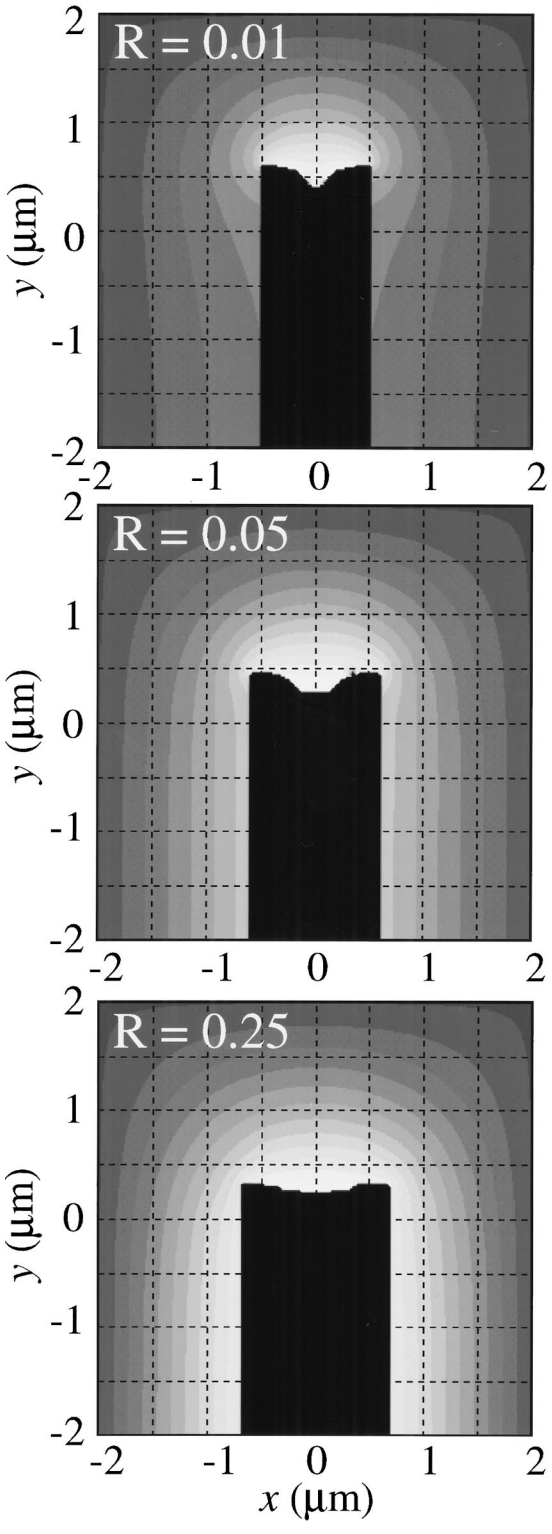

Fig. 6. Effect of the ratio R of the interfacial reaction constant K and diffusion constant/diffusion distance $D_l/\Delta x$. Simulations are performed changing the ratio $R = K/(D_l/\Delta x)$ from 0.01 (top) to 0.05 (middle) to 0.25 (bottom). All results are obtained after 40 000 s.

due to the non-saturated, saturated, and supersaturated liquids, respectively.

2. Concavity at the tip surface is a function of crystal width.
3. Strong growth anisotropy of the β-Si_3N_4 crystal (the interfacial reaction and diffusion controlled kinetics of the (100) and (001) surfaces, respectively), and supersaturation in the liquid phase must be satisfied for the development of concavity at the tip surface of the β-Si_3N_4 crystal.

REFERENCES

1. Lange, F. F., *J. Am. Ceram. Soc.*, 1973, **56**(10), 518.
2. Lange, F. F., *J. Am. Ceram. Soc.*, 1979, **62**(7–8), 428.
3. Hwang, C. M., Tien, T. -Y. and Chen, I. -W., in *Sintering '87*. ed. S. Somiya, M. Shimada, M. Yoshimura and R. Watanabe, Elsevier Applied Science, London, 1988, p. 1034.
4. Hwang, C. M. and Tien, T. -Y., *Mater. Sci. Forum*. 1989, **47**, 84.
5. Mitomo, M., Tsutsumi, M., Tanaka, H., Uenosono, S. and Saito, F., *J. Am. Ceram. Soc.*, 1990, **73**(8), 2441.
6. Mitomo, M. and Uesono, S., *J. Mater. Sci.*, 1993, **26**, 3940.
7. Einarsrud, M. -A. and Mitomo, M., *J. Am. Ceram. Soc.*, 1993, **76**(6), 1624.
8. Lai, K. -R. and Tien, T. -Y., *J. Am. Ceram. Soc.*, 1993, **76**(1), 91.
9. Han, S. -M. and Kang, S. -J. L., *J. Am. Ceram. Soc.*, 1993, **76**(12), 3178.
10. Lee, D. -D., Kang, S. -J. L. and Yoon, D. N., *J. Am. Ceram. Soc.*, 1988, **71**(9), 803.
11. Krämer, M., Hoffmann, M. J. and Petzow, G., *Acta metall. mater.*, 1993, **41**(10), 2939.
12. Krämer, M., Hoffmann, M. J. and Petzow, G., *J. Am. Ceram. Soc.*, 1993, **76**(11), 2778.
13. Petzow, G., Hoffmann, M.J., *Mater. Sci. Forum*. 1993, **113–115**, 91.
14. Hoffmann, M. J., in *Tailoring of Mechanical Properties of Si_3N_4 Ceramics*. ed. M. J. Hoffmann and G. Petzow, Kluwer Academic, Netherlands, 1994, pp. 59–72.
15. Wallace, J.S., Kelly, J.F., *Key Engineering Mater.*, 1994, **89–91**, 501.
16. Krämer, M., Wittmüss, D., Küppers, H., Hoffmann, M. J. and Petzow, G., *J. Crystal Growth*. 1994, **140**, 157.
17. Kitayama, M., Hirao, K., Toriyama, M. and Kanzaki, S., *Acta mater.*, 1998, **46**(18), 6541.
18. Kitayama, M., Hirao, K., Toriyama, M. and Kanzaki, S., *Acta mater.*, 1998, **46**(18), 6551.
19. Wötting, G. and Ziegler, G., *Ceram. Int.*, 1984, **10**(1), 18.
20. Wötting, G., Kanka, B. and Ziegler, G., in *Non-Oxide Technical and Engineering Ceramics*. ed. S. Hampshire, Elsevier Applied Science, London, 1986, p. 83.
21. Ziegler, G., Heinrich, J. and Wötting, G., *J. Mater. Sci.*, 1987, **22**, 3041.
22. Kleebe, H. -J., Pezzptti, G. and Ziegler, G., *J. Am. Ceram. Soc.*, 1999, **82**(7), 1857.
23. Krämer, M., Wittmüss, D., Küppers, H., Hoffmann, M. J. and Petzow, G., *J. Crystal Growth*. 1994, **140**, 157.
24. For example, Porter, A. D., Easterling, K. E., in *Phase Transformations in Metals and Alloys*. 2nd Ed. Chapman and Hall, London, 1992, p. 283.
25. Wang, L. -L., Tien, T. -Y. and Chen, I. -W., *J. Am. Ceram. Soc.*, 1998, **81**(10), 2677.
26. Taylar, J. E., *Acta Metall. Mater.*, 1992, **40**(7), 1475.
27. Babini, G. N., Bellosi, A. and Vincenzini, P., *Mater. Chem. Phys.*, 1984, **11**, 365.
28. Kaufmann, L., Hayes, F. and Birnie, D., *Calphad.*, 1981, **5**, 163.
29. Greenwood, G. W., *Acta Metall.*, 1956, **4**, 243.